

COBEM-2017-0666

ON THE ABSOLUTE INSTABILITY OF LAMINAR SEPARATION BUBBLES

Mateus Peixoto Avanci

Daniel Rodríguez

Leonardo Santos de Brito Alves

Graduate Program in Mechanical Engineering (PGMEC), Universidade Federal Fluminense, Niterói, RJ, Brazil
mateuspeixoto@id.uff.br, danielrodriguez@id.uff.br, leonardo.alves@mec.uff.br

Abstract. *Laminar separation bubbles occur due to separation, transition, and turbulent reattachment of the boundary-layer flow under adverse pressure gradients. They can appear in many practical flows, as aircraft airfoils or turbine blades. The stability characteristics of separation bubbles are studied here using the Orr-Sommerfeld equation and its inviscid analogous, the Rayleigh's equation. Base flow velocity profiles are modelled by a modified hyperbolic tangent function, and characterized with respect to their maximum reverse flow and the distance from the inflection point to the wall. Linear stability theory (LST) was used to identify the transition from convective to absolute character of Kelvin-Helmholtz instability. Two complementary approaches are used, namely a matrix-forming one based on spatial discretization of the equations using a spectral method that allows for the computation of the complete eigenspectra, and a shooting method for Rayleigh's equation that makes the parametric study very efficient.*

Keywords: *Laminar separation bubble, Boundary layer separation, Absolute/convective instability*

1. INTRODUCTION

Flow separation occurs in many nature and technological applications. For example, flow separation on airfoils occurring as the angle of attack is increased can cause important deviations of the lift vs. angle of attack curve, leading to an increase in the drag for the same flight condition. Failure of the detached boundary layer to reattach within a short distance from the separation point usually implies a sudden loss of lift and the appearance of important pitching moments, conditions known as stall. In other technological applications, like wind turbines, flow separation not only has a detrimental impact on the aerodynamic properties but also in the aeroacoustic noise generation. Flow separation has in general a negative impact on performance and for this reason is one of the main concerns in aerodynamic studies.

Under the influence of a sufficiently strong adverse pressure gradient, the boundary layer separates from the surface. If the Reynolds number is low enough the boundary layer at separation is laminar. The separated shear layer is known to be highly unstable with respect to the inflectional Kelvin-Helmholtz mechanism, and eventually transitions from the laminar to the turbulent regime. Finally, the strong mixing provided by the turbulence causes the separated layer to reattach, enclosing a re-circulation region usually referred to as laminar separation bubble (LSB). Low-turbulence wind-tunnel observations show that laminar-turbulent transition is mainly dominated by convective amplification of pre-existing instability waves in the attached boundary layer, whose amplitude is amplified by orders of magnitude due to the inflectional mean velocity profile. The flow around the separation location is steady whereas the flow near the reattachment location is highly unsteady, presenting shedding of three-dimensional vortical structures from the rear portion of the bubble. Intriguingly, an almost identical transition scenario is recovered in direct numerical simulations in which the convective inflectional instability is neglected by prescribing undisturbed inlet conditions. Consequently, a different and self-sustained instability mechanism must be acting on LSBs, that triggers unsteadiness and transition to turbulence even in the absence of external disturbances.

One such a possible mechanism is the inflectional instability itself, if the bubble's reversed flow portion is intense enough to sustain absolute instability, i.e. temporal growth of upstream-propagating disturbance waves. Different studies in the past analyzed this possibility. Allen and Riley (1995) described an investigation into the properties associated with small, two-dimensional separation bubbles. For such bubbles, laminar flow separation is not accompanied by laminar reattachment if the Reynolds number is sufficiently high. In that case, if reattachment is to take place, it must be as a turbulent flow. One of the main aims of this investigation is to determine the mechanism by which transition to turbulence may take place, in separated flows of such small extent, when the flow is subjected to a wall disturbance localized in time and space. However, they concluded that recirculation regions more intense than the ones present in their calculations were

required for absolute instability to appear. Using modified Falkner-Skan velocity profiles with reversed flow, Hammond and Redekopp (1998) examined a family of profiles in order to analyzed for the onset of absolute instability as the magnitude of the reversed flow increase, concluding that recirculations of at least 30% of the free-stream velocity were required. Another work of interest is Rist and Maucher (2002), which focuses on the analysis of parameters as wall distance of the inflection point, intensity of the shear layer, reverse-flow velocity and local Reynolds number in a possible absolute instability within a temporal instability approach; they lower the threshold for absolute instability to 30% of the free-stream velocity. More recently Diwan (2009) studied the dynamics of early stages of transition associated with laminar separation bubbles from a combined experimental and theoretical approach. He further reduced the reversed-flow threshold for absolute instability to a smaller 16%. Finally, Rodríguez *et al.* (2013) studied a family of LSB flows with peak reversed flows lower than 13% concluding that no absolute inflectional instability was present for the bubbles considered, while a three-dimensional stationary instability was already active for peak reversed flows as low as 7%, suggesting a different transition mode.

Interestingly, all the referenced studies considered different families of base flows and even if they allowed for variations in the wall-normal extent of the reversed flow region, they concentrated their analyses on the peak reversed flow. This opens the possibility of an even reduced critical reversed flow for self-sustained instability if the wall-normal extent of the bubble is varied appropriately. The present study starts from a inviscid analysis with Rayleigh's equation and a hyperbolic tangent velocity profile such a Dovgal *et al.* (1994). The analytic profile is used to construct generic models of separation bubbles and study the possible onset of local absolute instability in the representative spatially-developing flows in order to verify whether or not the peak recirculation is the only parameter of interest.

2. METHODOLOGY

2.1 Linear Stability Theory

The calculations are based on the usual assumptions for Linear Stability Theory of incompressible fluids: parallel-flow approximation, small-amplitude disturbances and normal disturbance modes, i.e., a decomposition of the total flow-field as Eq. (1).

$$\mathbf{q}(x, y, t) = \bar{\mathbf{q}}(y) + \epsilon \mathbf{q}'(x, y, t) \quad (1)$$

Here $\bar{\mathbf{q}}(y) = \bar{u}(u)$ is the base flow profile, $\mathbf{q}'(x, y, t) = [u', v', p']^T$ is the vector of disturbance fluid variables, ϵ is the linearly-small disturbance amplitude, x is the streamwise coordinate, y is the wall-normal coordinate and t is time.

2.2 Orr-Sommerfeld/Rayleigh

To theoretically investigate stability characteristics of locally-parallel LSB profiles, modal analyses using both the Orr-Sommerfeld and Rayleigh equations have been performed. The Orr-Sommerfeld equation is an eigenvalue equation describing the viscous linear two-dimensional instability modes of a parallel flow and it is given by Eq. (2). See Drazin and Reid (2004).

$$\left(\bar{u} - \frac{\omega}{\alpha}\right)(\phi'' - \alpha^2\phi) - U''\phi = \frac{1}{i\alpha Re}(\phi^{iv} - 2\alpha^2\phi'' + \alpha^4\phi) \quad (2)$$

The prime (') indicates differentiation with respect to y . All the quantities are non-dimensionalized using appropriate parameters. Thus, α is a streamwise wave number and ω is a the complex frequency, Re is the Reynolds number and i the imaginary number. $\phi(y)$ is the complex amplitude of the disturbance streamfunction which is directly proportional to the transverse disturbance velocity v , and is related to the streamwise disturbance velocity by

$$u(x, y, t) = -\frac{1}{i\alpha}\phi(y)e^{i(\alpha x - \omega t)} + c.c. \quad (3)$$

The inviscid Kelvin-Helmholtz instability being dominant for LSBs, the simpler Rayleigh's equation is expected to deliver results comparable to those of the complete Orr-Sommerfeld equation for this class of base flows. Rayleigh's equation is obtained by neglecting the viscous term in the Orr-Sommerfeld's equation, Eq. (2), and is given by Eq. (4).

$$\left(U - \frac{\omega}{\alpha}\right)(\phi'' - \alpha^2\phi) - U''\phi = 0 \quad (4)$$

The simpler form of Rayleigh's equation allows us to perform a large parametric study in a reasonable time. The validity of the inviscid approximation for the determination of the critical conditions for absolute instability is studied in subsection (3.1).

The modified hyperbolic tangent profile proposed by Dovgal *et al.* (1994) is used here to construct a wide variety of base flows representative of LSBs:

$$\bar{u}(y) = [\tanh a(y - d) + \tanh ad]/(1 + \tanh ad) + b\sqrt{3}(y/d)\exp[-1.5(y/d)^2 + 0.5] \quad (5)$$

Here b is a measure of the magnitude of reversed flow and d is the non-dimensional distance of the inflection point from the wall. The constant a is chosen such that the momentum thickness is equal to one, i.e. Eq. (6) is satisfied.

$$\int_0^\infty U(y)(1 - U(y))dy = 1 \quad (6)$$

2.3 Numerical methods

Two different numerical methods for the solution of the locally-parallel eigenvalue problems described by the Orr-Sommerfeld and Rayleigh's equations are employed in this work. The first one is a matrix-forming approach, used for both equations, in which the differential operators are spatially discretized using a conveniently mapped Chebyshev-Gauss-Lobatto mesh. This results into a matrix eigenvalue problem, that is formed and stored in memory and solved numerically using the implementation of the QZ algorithm available in the open-source library LAPACK, as was first done by Orszag (1971).

The second method is based on the spatial marching of the governing equations from the free-stream towards the wall. For a prescribed wavenumber α , the value of ω is adjusted iteratively until the boundary conditions at the wall are satisfied. This second method, usually known as shooting method, is only used here for the solution of the inviscid Rayleigh's equation.

The results of both approaches are cross-validated for some representative cases. The matrix-forming method is also used in the comparison between viscous and inviscid analyses, in order to ascertain if viscosity plays an important role in the critical conditions for the onset of absolute instability. Finally, the matrix-forming results are also used to provide initial guesses for the shooting method, so the parametric studies can be initialized.

The determination of the absolute/convective nature of instability waves is based on the behavior of the waves with zero group velocity, i.e. $\frac{\partial \omega}{\partial \alpha} = 0$, as those waves do not propagate either upstream or downstream from their location of introduction. The zero group velocity condition is a saddle-point condition for the complex ω in the complex α plane, and its determination can be done following different approaches. Based on the results of the matrix-forming approach, a rectangular mesh in the α plane is mapped onto the ω plane, and the zero-group-velocity conditions are identified visually where the coordinate lines fold intersecting themselves into a cusp-point. Corresponding to this complex ω_0 , a saddle point is identified in the α plane, in which two branch solutions, α^+ and α^- intersect themselves in a saddle or pinching point. This procedure is tedious and not advisable for a large parametric study, as the one intended here; consequently a different and novel approach is used instead, described in the next section, and the one based on the identification of the cusp point is employed only for cross validations and providing the initial guesses.

2.4 Shooting method to determine pinch-point

The idea here is transform the boundary condition problem in a initial condition problem and solve a system of two complex equations that determine the dispersion relation involving the four variables α_r , α_i , ω_r and ω_i . Rayleigh's equation (4) is the first governing equation; a convenient second equation is obtained by differentiating Rayleigh's equation with respect to α :

$$\left[\left(U - \frac{\partial \omega}{\partial \alpha} \right) (\phi'' - \alpha^2) - 2\alpha(\alpha U - \omega) - U'' \right] \phi + [(\alpha U - \omega)(\phi'' - \alpha^2) - \alpha U_{yy}] \phi_\alpha = 0, \quad (7)$$

where ϕ_α is $\frac{\partial \phi}{\partial \alpha}$. With the objective of restricting the possible solutions to those with zero group velocity, $\frac{\partial \omega}{\partial \alpha} = 0$ is imposed implicitly in Eq. (7).

The system of equations is solved using a shooting method, marching from the free-stream towards the wall. "Initial" free-stream conditions need to be imposed to the real and imaginary parts of ϕ and ϕ_α , as well to their first derivatives:

$$\phi_\infty = 1, \quad \phi'_\infty = -i\alpha, \quad \phi_{\alpha\infty} = 0 \quad \text{and} \quad \phi'_{\alpha\infty} = 0. \quad (8)$$

The complex α and ω values are iterated with the aid of a Newton's method until the "final" wall conditions are satisfied:

$$Re(\phi_0) = 0, \quad Im(\phi_0) = 0, \quad Re(\phi_{\alpha 0}) = 0 \quad \text{and} \quad Im(\phi_{\alpha 0}) = 0. \quad (9)$$

The computed solutions verify Rayleigh's equation and boundary conditions and the zero-group-velocity condition, and thus corresponds automatically to saddle points in the complex α plane. The corresponding complex frequency and

Table 1: List of cases

Case	d	b
A1	3	-0.35
A2	3	-0.15
B1	5	-0.35
B2	5	-0.15
C1	9	-0.35
C2	9	-0.15

Table 2: Pinch-points for different configurations and Reynolds number

Case	Reynolds	Reynolds number			
		α_r	α_i	ω_r	ω_i
A1	300	0.4257	-0.1770	0.0654	0.0115
	600	0.4187	-0.1848	0.0657	0.0144
	∞	0.4228	-0.1649	0.0678	0.0205
A2	300	0.5014	-0.4474	0.1068	-0.0630
	600	0.4654	-0.4460	0.1052	-0.0599
	∞	0.4578	-0.4312	0.1020	-0.0531
B1	300	0.2678	-0.1329	0.0522	0.0048
	600	0.2670	-0.1277	0.0524	0.0063
	∞	0.2645	-0.1237	0.0532	0.0095
B2	300	0.2864	-0.2566	0.0860	-0.0324
	600	0.2841	-0.2611	0.0857	-0.0310
	∞	0.2854	-0.2545	0.0845	-0.0277
C1	300	0.1505	-0.0786	0.0346	0.0040
	600	0.1503	-0.0743	0.0349	0.0048
	∞	0.1528	-0.0757	0.0352	0.0061
C2	300	0.1770	-0.1484	0.0630	-0.0090
	600	0.1813	-0.1579	0.0630	-0.0080
	∞	0.1750	-0.1479	0.0629	-0.0072

wavenumber are referred to as the absolute frequency ω_0 and the absolute wavenumber α_0 . If the imaginary part of the absolute frequency is positive, then instability waves exist which grow in amplitude while they propagate upstream, i.e. the base flow profile is absolute unstable. Consequently, $Im(\omega_0) = 0$ determines the critical conditions for the onset of absolute instability.

3. RESULTS

3.1 Cross-validation of the Orr-Sommerfeld/Rayleigh solutions

The objective of this subsection is to show that viscosity does not play a relevant role in the inflectional instability at conditions close to the critical ones for the onset of absolute instability, and that consequently the inviscid analysis by means of the Rayleigh's is sufficient for the subsequent study. Six different base flows are considered for the validations, defined by the parameters shown in Tab. 1. The absolute frequency and wavenumber are calculated for inviscid ($Re \rightarrow \infty$) and two viscous conditions, $Re = 300$ and 600 , and the results are compared in Tab. 2, showing a good agreement in all cases.

The eigenfunctions corresponding to the four extreme cases considered, namely A1, A2, C1 and C2, as obtained by the viscous and inviscid analyses, are compared in Fig. 1. Except for a very thin layer in contact with the wall, in which the eigenfunctions adapt to the more restrictive no-slip boundary conditions for the viscous analysis, results from the Orr-Sommerfeld and Rayleigh's analysis are identical.

It is important to remark that all the cases considered are relatively close to the critical conditions for absolute instability, but important differences exist between the base flow properties, including peak reversed flow and wall-normal extent of the reversed flow. This builds confidence that the six base flows considered for the validation are general enough to demonstrate the validity of the inviscid analysis.

3.2 Description of the cases and additional cross-validations

In order to characterize the analytical solution for the base flow profile, two cases examples are presented in Fig. 2. One of them has a inflection point coordinate y_{inf} lower than that of the dividing point y_d , and the other base flow profile the contrary. Figures 3 and 4 show the dependence of the parameter h_R , which is the point where U is equal a zero, and the peak reversed flow U_R , with the base flow parameters b and d .

In the parametric study of the absolute/convective instability properties, the very first guess for the shooting method was taken as the most unstable mode from matrix forming method. In agreement with that, this subsection has the aim of validating the shooting method described in section 2.4 with results by the matrix-forming method. Figure 5 compares the solutions of the Rayleigh equation for the disturbance velocity component u for both methods.

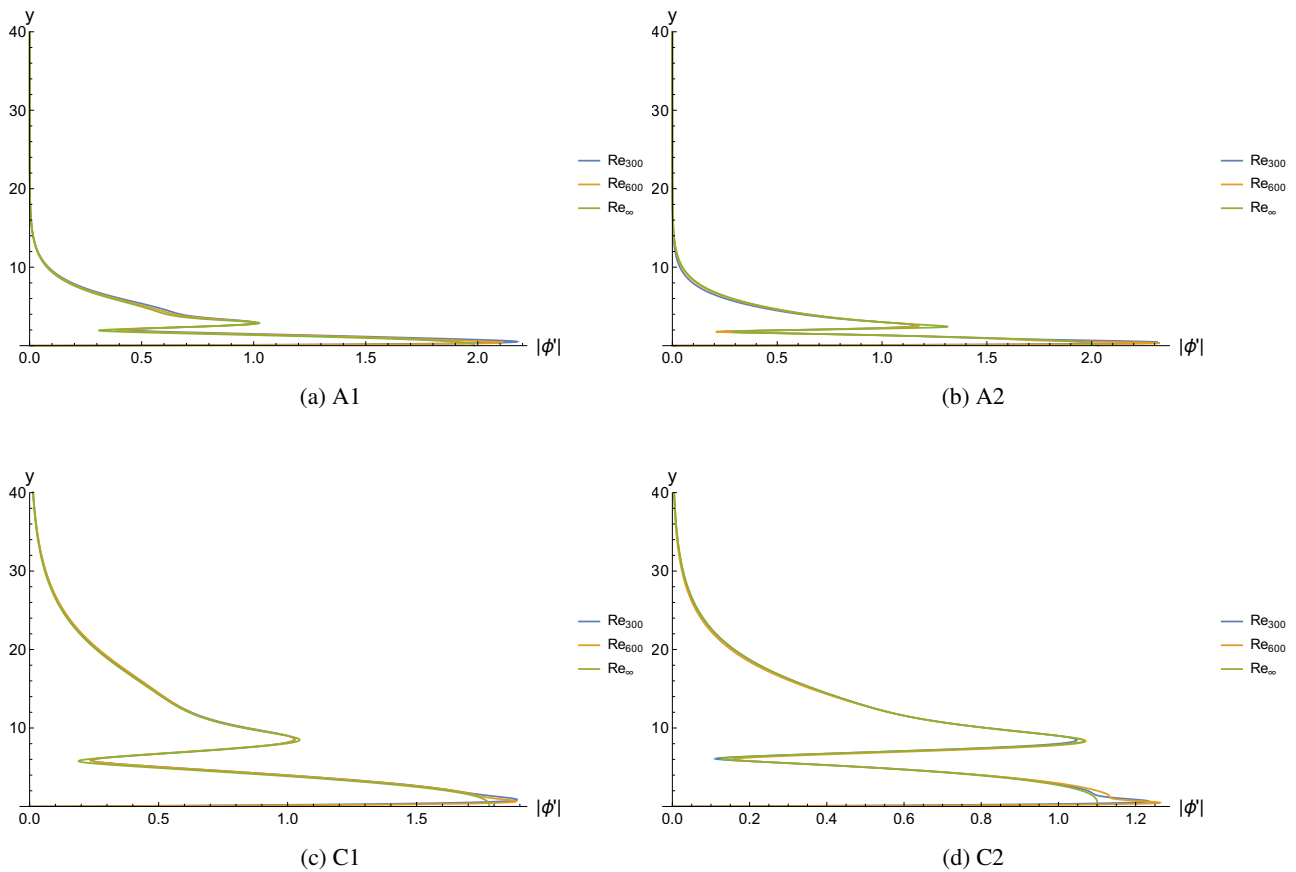


Figure 1: Eigenfunctions for four distinct parameters configuration varying the Reynolds number.

3.3 Absolute/Convective analyses

A large parametric study of the absolute frequency for varying base flows was performed using the validated shooting method from section 2.4. The results are shown in Fig. 6 and Fig. 7.

Here the red lines represent the critical curves for the convective/absolute instabilities, $Im(\omega_0) = 0$. We can observe that the peak reversed flow is in good agreement with the literature (Diwan (2009); Rist and Maucher (2002)) and is about 15% of the free-stream velocity. However, these results show that the reversed flow is not enough to determine if the configuration is convectively or absolutely unstable, and the wall-normal size of the reversed flow region, h_R , also must be taken into account. Figure 7 shows the variation of $Im(\omega_0)$ with the parameters d which represents the wall-normal coordinate of the inflection point, and b which represents the intensity of the reversed flow.

3.4 Dividing/Inflection point

In possession of the results the next step was mapping the pinch-points with the related inflection and dividing points. The Fig. 8 shows the results for just one value of inflection point, which coincides with the parameter d , with the variation of the parameter b . The aim was just to verify the value of b that is the intersection of the two curves and compare with the b found by Diwan (2009). The value of b found by Diwan (2009) was $b = -0.2478$ consistent with the results of the present work.

The mapping made with the pinch-points and the values of those two parameters y_{inf} and y_d , is shown in Fig. 9. In order to establish a relation between y_{inf} , y_d and the onset of the absolute instability we can plot the critical curve ($\omega_i = 0$) with respect to these parameters, which is shown in Fig. 10. The results show that for values $y_{inf} > y_d$ the inflectional instability is of convective nature, while for $y_{inf} < y_d$ absolute instability is recovered in all cases.

4. CONCLUSIONS

This paper addressed the origin of self-sustained oscillations in LSB flows by means of locally-parallel linear stability analyses of velocity profiles representative of boundary layers with reversed flow. Two different methodologies for the study of the absolute/convective nature of plane waves were cross-validated, one based on the classic matrix-forming approach and cusp-point method, and the other on an extension of the shooting solution method that automatically recovers

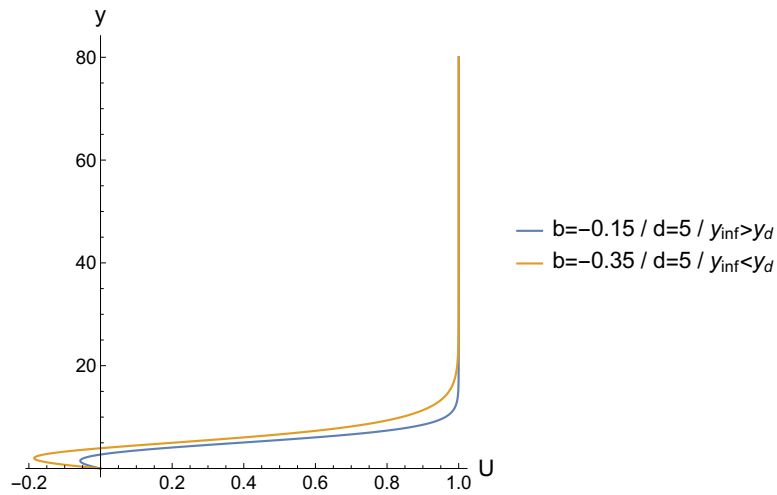


Figure 2: Two base flow profiles are showing following Dovgal *et al.* (1994).

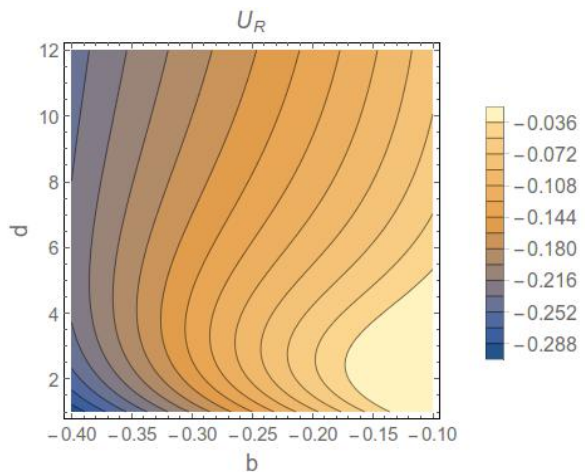


Figure 3: Variation of the maximum reverser flow velocity with the parameters d and b .

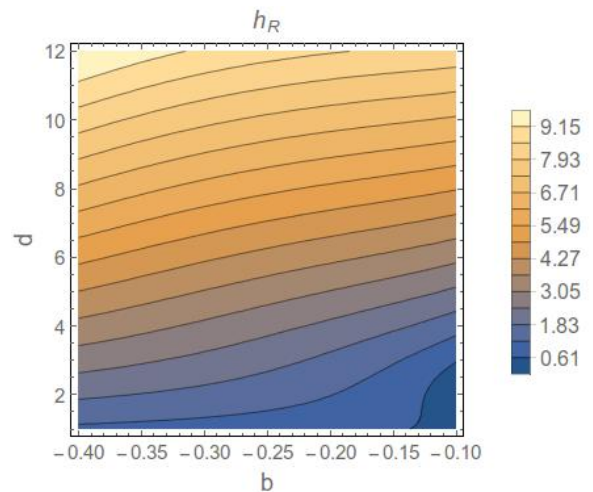


Figure 4: Variation of the point where velocity is equal a zero with the parameters d and b .

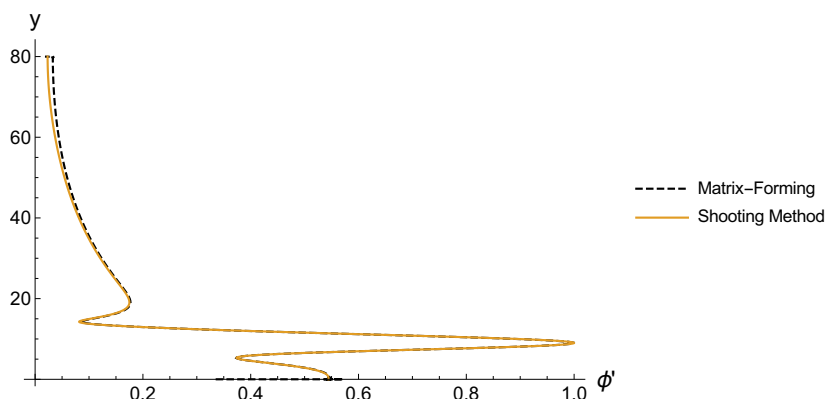


Figure 5: Auto-functions performed by Matrix-forming and Shooting method. $d = 9$ and $b = -0.15$.

the correct absolute frequency and wavenumber corresponding to the zero group velocity perturbations. The use of the second methodology allow for performing a very large parametric study, with the objective of determining the base flow parameters relevant for the onset of absolute instability.

Present results show that the critical conditions for absolute instability are not solely dependent on the peak reversed flow, but also on the wall-normal extent of the reversed flow region. The threshold of 16% found in the literature corresponds to an upper bound, and reductions in this value up to 12-13% are observed for LSBs particularly thin. Whether this kind of LSBs can be realizable in experiments or not is a different question that should be addressed in the future

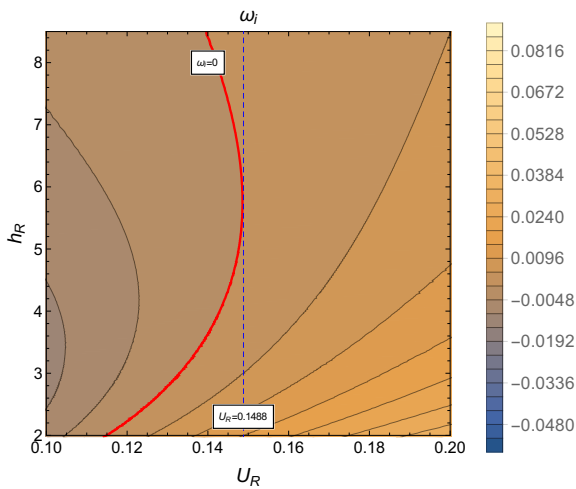


Figure 6: Variation of ω_i with the parameters U_R and h_R .

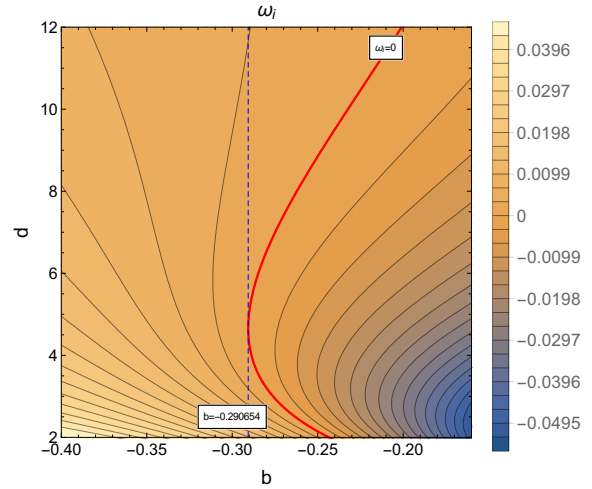


Figure 7: Variation of ω_i with the parameters d and b .

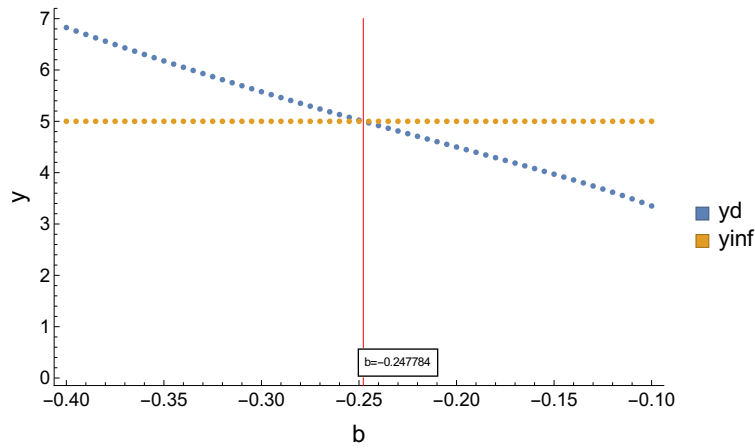


Figure 8: Variation of y_{inf} and y_d with b for $d = 5$.

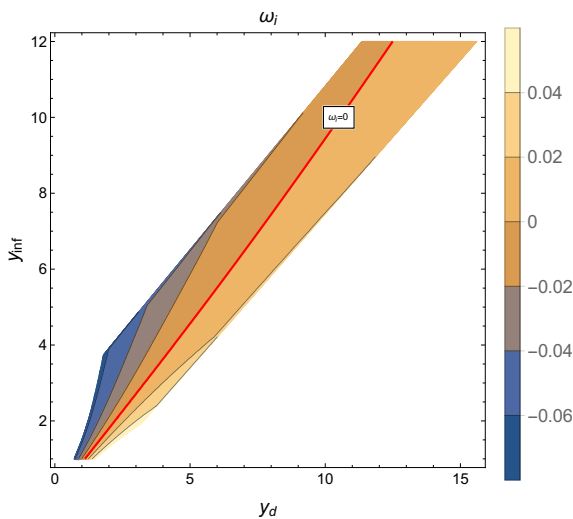


Figure 9: Mapping with the parameters y_{inf} and y_d with ω_i .

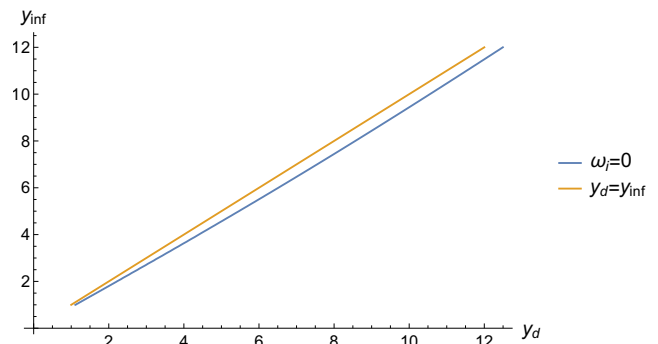


Figure 10: The critical curve ($\omega_i = 0$) with the variation of y_{inf} and y_d .

by means of comprehensive literature surveys. Following the suggestion made by Diwan (2009), the relation between the absolute/convective instability and the relative coordinates of the base flow's inflection point and dividing streamline was monitored. It is found that when the inflection point lies within the reversed flow region, absolute instability should be expected, while an inflection point outside implies convective instability. The physical cause and implications of this

finding is currently under investigation.

5. ACKNOWLEDGEMENTS

The first author's work is funded by a CNPq post-graduate scholarship, within the Postgraduate program in Mechanical Engineering (PGMEC/UFF). This work is supported by CNPq grants 405144/2016-4 and 305512/2016-1.

6. REFERENCES

- Allen, T. and Riley, N., 1995. "Absolute and convective instabilities in separation bubbles". *The Aeronautical Journal*, Vol. 99, No. 990, pp. 439–449.
- Diwan, S., 2009. *Dynamics of early stages of transition in a laminar separation bubble*. Ph.D. thesis, PhD thesis, Indian Institute of Science, Bangalore, India.
- Dovgal, A., Kozlov, V. and Michalke, A., 1994. "Laminar boundary layer separation: instability and associated phenomena". *Progress in Aerospace Sciences*, Vol. 30, No. 1, pp. 61–94.
- Drazin, P.G. and Reid, W.H., 2004. *Hydrodynamic stability*. Cambridge university press.
- Hammond, D.A. and Redekopp, L.G., 1998. "Local and global instability properties of separation bubbles". *European Journal of Mechanics-B/Fluids*, Vol. 17, No. 2, pp. 145–164.
- Orszag, S.A., 1971. "Accurate solution of the orr–sommerfeld stability equation". *Journal of Fluid Mechanics*, Vol. 50, No. 4, pp. 689–703.
- Rist, U. and Maucher, U., 2002. "Investigations of time-growing instabilities in laminar separation bubbles". *European Journal of Mechanics-B/Fluids*, Vol. 21, No. 5, pp. 495–509.
- Rodríguez, D., Gennaro, E.M. and Juniper, M.P., 2013. "The two classes of primary modal instability in laminar separation bubbles". *Journal of Fluid Mechanics*, Vol. 734.

7. RESPONSIBILITY NOTICE

The author(s) is (are) the only responsible for the printed material included in this paper.